Diffuse Reflectance Spectroscopy for Surface Measurement of Liver Pathology

NILSSON, JAN; Reistad, Nina; Brange, Hannes; Öberg, Carl-Fredrik; Sturesson, Christian

Published in:
European Surgical Research

DOI:
10.1159/000449378

2016

Document Version:
Peer reviewed version (aka post-print)

Diffuse reflectance spectroscopy for surface measurement of liver pathology

Running head: DRS for liver surface measurement

Jan H Nilsson[a], Nina Reistad[b], Hannes Brange[a], Carl-Fredrik Öberg[a] and Christian Sturesson[a]

[a] Lund University, Skane University Hospital, Department of Clinical Sciences Lund, Surgery, Lund, Sweden

[b] Department of Physics, Lund University, Lund, Sweden

Category: Original article

Corresponding author

Christian Sturesson

Department of Surgery

Skåne University Hospital

S-221 85 Lund

Sweden

e-mail: christian.sturesson@med.lu.se

tel: +46-46-172347

fax: +46-46-172335

Abstract

Background: Liver parenchymal injuries such as steatosis, steatohepatitis, fibrosis and sinusoidal obstruction syndrome can lead to increased morbidity and liver failure after liver resection. Diffuse reflectance spectroscopy (DRS) is an optical measuring method that is fast, convenient and established. DRS has previously been used on the liver with an invasive technique consisting of a needle that is inserted into the parenchyma. We have developed a DRS system with a hand-held probe that is applied to the liver surface. In this study we have investigated the impact of the liver capsule on DRS measurements and whether liver surface measurements are representative of the whole liver. We also wanted to confirm that we could discriminate between tumor and liver parenchyma with DRS.

Materials and methods: The instrumentation setup consisted of a light source, a fiber optic contact probe, and two spectrometers connected to a computer. Patients scheduled for liver resection due to hepatic malignancy were included, and DRS measurements were performed on the excised liver part with and without the liver capsule and alongside a new cut surface. To estimate the scattering parameters and tissue chromophore volume fractions, including blood, bile and fat, the measured diffuse reflectance spectra were applied to an analytical model.

Results: In total, 960 DRS spectra from the excised liver tissue of 18 patients were analyzed. All analyzed factors regarding tumor versus liver tissue were significantly different. When measuring through the capsule, blood volume fraction was found to be 8.4±3.5%, lipid volume fraction was 9.9±4.7% and bile volume fraction was 8.2±4.6%. No differences could be found in surface measurements compared to cross-section measurements. In measurements with/without the liver capsule the differences in volume fractions were for blood, lipid and bile 1.63 (0.75 - 2.77)%, -0.54 (-2.97 - 0.32)% and -0.15 (-1.06 - 1.24)%, respectively.

Conclusion: This study shows that it is possible to manage DRS measurements through the liver capsule and that surface DRS measurements are representative of the whole liver. The results are consistent with earlier published data on the combination of liver chromophores. The results encourage us to proceed with in-vivo measurements for further quantification of liver composition and assessment of parenchymal damage such as steatosis and fibrosis grade.

Key words

DRS, liver capsule, liver surgery, optical measurements, steatosis

Introduction

In liver surgery, assessment of parenchyma characteristics is valuable when considering the resectability of liver tumors. Liver parenchymal injuries due to chronic liver disease and preoperative chemotherapy can lead to increased morbidity and liver failure after liver resection [1-3]. Although steatosis can be detected non-invasively with magnetic resonance imaging, and liver fibrosis can be evaluated with elastography, histological analysis of a liver biopsy remains the gold standard for assessing the degree of steatosis, fibrosis and steatohepatitis [4-6]. Sinusoidal obstruction syndrome is a chemotherapy-induced liver damage that is difficult to discover preoperatively [7]. As a predictive marker, volumetric changes of the spleen size have been suggested for identification of sinusoidal obstruction syndrome [8]. However, at the time of surgery, previously unknown liver damage may be found or suspected, calling for methods for intraoperative identification and quantification of this damage.

Diffuse reflectance spectroscopy (DRS) is an optical measuring method that is fast, convenient and relatively established, and is used in different areas as lung, breast, skin and gut [9-13]. The tissue is illuminated with light from a broadband light source and the diffusely reflected light, after interacting with the tissue, is collected and analyzed. By fitting the analyzed data to a mathematical model, tissue characteristics such as structure and composition can be estimated.

Evers et al. have shown promising results using DRS in liver tissue in both ex-vivo and in-vivo clinical studies where they have demonstrated high accuracy in discriminating between liver and tumor parenchyma, and also the possibility to quantify parenchyma compounds such as steatosis [14-16]. However, their equipment consists of a fiber optic needle that is inserted into the parenchyma, which could be problematic to implement in a clinical setting.

Therefore, the aim of the present study was to develop a DRS system with a hand-held

custom-made probe applied to the liver surface. As the penetration depth of light is limited to a few mm in liver tissue, surface measurements are limited to the most superficial part of the liver and require measurements through Glisson's capsule. Glisson's capsule is the membrane covering the liver surface and is made up of elastin and collagen fiber networks [17]. The impact on Glisson's capsule on DRS measurements was investigated. Because of the short penetration depth of light, it is necessary to examine whether liver surface measurements are representative of the whole liver. Additionally, we wanted to confirm that we could discriminate between tumor and liver parenchyma with DRS.

Materials and Methods

DRS system

The instrumentation setup consisted of a light source, a fiber optic contact probe, a probe cylinder and two spectrometers connected to a computer with computer software for data collection (Fig. 1). A Tungsten-Halogen light source (Ocean Optics HL-2000-HP, Ocean Optics, FL, USA) was used emitting light from around 360 to 2000 nm through a custom-designed 10 mm diameter trifurcated fiber bundle probe attached to a 25 mm probe cylinder, thereby minimizing pressure effects, stabilizing the probe, and removing the impact of ambient light. The fiber bundle consisted of a single 400 μm diameter illuminating fiber in the center and ten collecting 200 μm diameter fibers placed in a ring with a source-detector separation of 2.5 mm. A close-up image of the probe top is shown in Fig. 2. Every other collecting fiber was connected to a spectrometer in the visible wavelength range (Ocean Optics QE6500-VIS-NIR, Ocean Optics, FL, USA) and the others were connected to a spectrometer in the near infrared range (Ocean Optics NIRQuest512, Ocean Optics, FL, USA). Using these two spectrometers simultaneously, spectra were obtained in the range 400–1600 nm. To control the spectrometers and acquire data, computer software (Ocean-View, Ocean Optics, FL, USA) was used on a standard personal computer laptop.

Mathematical model

The wavelength dependence of scattering was described in terms of the separate contributions of Rayleigh and Mie scattering at a reference wavelength (λ_0) set to 800 nm, $\mu_s'(\lambda) = \mu_s'(\lambda_0)(\rho(\lambda/\lambda_0)^{-b} + (1-\rho)(\lambda/\lambda_0)^{-4})$, where the scaling factor $\mu_s'(\lambda_0)$ corresponds to the reduced scattering amplitude at this specific wavelength, b the Mie scattering slope and ρ denotes the Mie-to-Rayleigh fraction of scattering [18].

In liver tissue the absorption in the visible wavelength range is dominated by hemoglobin and bile, whereas water, lipid and collagen are the main absorbers in the near infrared wavelength range [14,19,20]. The blood related absorption is represented through the effective absorption coefficient for a volume of tissue containing blood vessels as $\mu_a^{Blood}(\lambda) = C(\lambda)c_{HbT}\mu_a^{HbT}(\lambda)$, where c_{HbT} is the total hemoglobin volume fraction, StO_2 is the level of hemoglobin oxygen saturation, and $\mu_a^{HbT}(\lambda) = StO_2\mu_a^{HbO_2}(\lambda) + (1-StO_2)\mu_a^{Hb}(\lambda)$. $\mu_a^{HbO_2}(\lambda)$ and $\mu_a^{Hb}(\lambda)$ correspond to the absorption coefficients of fully oxygenated and deoxygenated whole blood, given an average hemoglobin concentration of 150 mg/ml. The pigment packaging factor ($C(\lambda)$) was used to account for inhomogeneous distribution of hemoglobin in vessels [21] and is a function of the average vessel optical density $C(\lambda) = \left(1 - e^{-2R\mu_a^{HbT}(\lambda)}\right)/\left(2R\mu_a^{HbT}(\lambda)\right)$, where *R* corresponds to the average vessel radius. Furthermore, as suggested by Nachabe et al. [22], the absorption coefficients of lipid ($\mu_a^{Lipid}(\lambda)$) and water ($\mu_a^{Water}(\lambda)$) were combined to avoid covariance since both substances absorb light over the same wavelength range, resulting in a more stable fit $\mu_a^{WL}(\lambda) = c_{WL}\left[f_{Lipid}\mu_a^{Lipid}(\lambda) + (1-f_{Lipid})\mu_a^{Water}(\lambda)\right]$. The coefficients c_{WL} and f_{Lipid} represent the total volume fraction of water and lipid in the probe volume and the lipid fraction within this volume, respectively. Finally, the absorption due to bile and collagen is represented as $\mu_a^{Other}(\lambda) = c_{Bile}\mu_a^{Bile}(\lambda) + c_{Collagen}\mu_a^{Collagen}(\lambda)$, where $c_{Bile}$and $c_{Collagen}$are the bile and collagen volume fractions respectively. Using

available absorption spectra from the literature [19,23-28] as a priori knowledge to the model, we assume that the linear combination $\mu_a^{Tissue}(\lambda) = \mu_a^{Blood}(\lambda) + \mu_a^{WL}(\lambda) + \mu_a^{Other}(\lambda)$ can fully approximate the absorption coefficient within the liver tissue volume probed by the light.

Clinical design

The regional ethics committee approved the study protocol (Dnr2014/788), and oral and written informed consent was obtained from all patients. Patients scheduled for liver resection due to hepatic malignancy were included. DRS measurements were incorporated in the standard liver resection surgery procedure and were performed on the excised liver section within 10 minutes after resection. The light source and the spectrometers were left on for at least 15 minutes to warm up prior to measurements. A background spectrum was acquired by simply shutting off the light input and thereafter measuring the output signal from each pixel with no light incident onto the two detectors. To record the spectral power distribution of the light source, the wavelength-dependent response of the instrument, and the throughput of the fiber optic probe, an intensity calibration spectrum was measured on a spectrally flat white reflectance standard (Spectralon SRS-99-010, Labsphere, Inc., USA). The calibration and measurement procedures used the same integration time and the procedure was designed to provide backscattered light in the same order of magnitude as liver tissue, enabling fixed integration times. Background and intensity calibration spectra were recorded before and after a set of tissue measurements. The probe, including approximately 2m of the fiber cable system, was encased in sterile foil (Video camera laser drape, Microtek Medical B.V., Zutphen, The Netherlands). Measurements were first made directly on the liver parenchyma with an intact capsule followed by measurements on approximately the same position after the capsule had been removed. Secondly, a new cut surface was made through the macroscopically normal tissue perpendicular to the liver surface and measurements were

obtained in series following sequences of 5 mm starting from 0 mm up to a maximum of 30 mm depending on tissue thickness. Finally, measurements were made directly on tumor tissue. The size of the excised liver section greatly varied resulting in that the number of measurements that could be made on each specimen also varied. Each collected DRS spectrum was made up from the average of ten different measurements, five from each spectrometer. After DRS measurements, the excised liver tissue was fixed in 4% formalin for histological analysis which was later performed by a pathologist, using hematoxylin and eosin stain and trichrome stain. Steatosis was classified according to D'Alessandro et al. [29]. To rescale the lipid volume fraction to the area fraction used by the pathologist, the following formula was used: $Lipid_{volume} = \frac{4}{3\sqrt{\pi}}(Lipid_{area})^{3/2}$ [15,30].

Data analysis

All raw tissue spectra as well as the intensity calibration spectrum were background corrected by subtracting the acquired background spectrum. Diffuse reflectance spectra were thereafter calculated through standard intensity normalization. To form continuous spectra from 400 to 1600 nm, the overlapping wavelength region of the two spectrometers was used to compute a merging factor. The merging factor depends on the optical contact state between the probe and the tissue as well as on the homogeneity of the probe volume and should ideally be equal to one. To estimate the scattering parameters and chromophore volume fractions of the probed tissue volume, the measured diffuse reflectance spectra were applied over the wavelength range from 550 to 1450 nm with the analytical model introduced by Farrell et al. [31]. The applicability of this single source analytical light propagation model, derived from diffusion theory, is a well-studied and validated inverse problem that requires the distance between the emitting and collecting fibers at the tip of the probe as well as known wavelength-dependent absorption coefficients of the relevant chromophores as input arguments [31-34]. The tissue

regions from which the spectra were derived were assumed to be optically homogeneous, a standard non-linear least squares fitting algorithm available in the MatLab software package (MathWorks Inc., Natick, MA) was applied and the method described by Amelink et al. [35] to assess the reliability of the estimated parameters was used. Quantitative estimates of the scattering and absorption parameters were revised iteratively to minimize the difference between the spectrum generated by the model and that acquired from the liver tissue.

Statistical analysis

Results are expressed as mean (standard deviation) or median (interquartile range). A Mann-Whitney *U*-test was used to compare continuous data, and related samples were compared with a Wilcoxon signed-rank test. A $p<0.05$ was considered statistically significant. Statistical analysis was performed using IBM SPSS Statistics version 22 (IBM, Armonk, NY, USA).

Results

Analysis was conducted on 960 DRS spectra from 192 measurement points, from 18 patients' excised liver tissue. Capsular measurements were made on 15 patients, depth measurements on 11 patients and tumor measurements on 15 patients. Fifty-four out of the total 192 measurement points were made on tumor tissue. Patient characteristics are shown in Table 1. Typical DRS spectra as a function of wavelength for with/without capsule, surface/cross-section and tumor/healthy liver tissue are shown in Fig. 3. Fig. 4 shows boxplots of DRS factors for tumor versus healthy liver tissue. All analyzed factors regarding tumor versus liver tissue were statistically significantly different. In Table 2, relevant model analysis results regarding capsule versus no capsule and surface versus cross-section measurements are shown. In all through capsule measurements, blood volume fraction was found to be 8.4±3.5%, lipid volume fraction 9.9±4.7% and bile volume fraction 8.2±4.6%. All included patients had histological steatosis grade 0 or 1 and no patient had significant fibrosis.

Discussion

In this study, a new method to perform surface measurements on human liver is presented. Making surface DRS measurements of the liver with a hand-held probe is a, to the liver, non-invasive technique that ultimately is intended to be used to evaluate liver parenchymal damage in real time. By making surface measurements on multiple sites, the method is less sensitive to sampling error as is the case with biopsy [36]. Evers et al. made DRS measurements on human liver by using an invasive technique with a fiber optic needle. This should be equated with needle biopsy where hemorrhage is a potential adverse event [37]. Thus, a surface measurement is preferable. Surface DRS probes have been used in several settings [12,38], but never in measurements of internal organs of humans. In this study, non-invasive DRS measurements with a surface probe on resected liver specimens originating from 18 patients were made.

Our measurements were applied to an analytical model that has been used by others in similar settings [16,31,33,39]. When measuring on the liver surface through Glisson's capsule, the volume fraction values found were 8.4% blood, 9.9% lipid and 8.2% bile. This lipid volume fraction is equivalent to a lipid area fraction of 5.6%, reflecting the low steatosis grade of the included patients. The values are also consistent with previous results using similar technology [14,16].

In a previous study on human hepatic microcirculation with a hand-held microscope, the liver capsule had to be removed to allow measurements [40]. The impact of the capsule was therefore particularly interesting to evaluate when measuring with DRS. In this study, measurements through the liver capsule resulted in a slightly reduced, but consistent, diffuse reflectance in the visible wavelength range and no influence in the near infrared range (Fig. 3). The shape of the spectra was not affected. Apart from blood volume fraction, which was

found to be somewhat greater with the capsule intact, no difference could be found in liver parenchyma composition when measuring through the liver capsule compared to without liver capsule (Table 2). The difference in blood volume could be related to the process of removing the capsule, which inevitably involved removing some subcapsular blood.

The penetration depth in our DRS measurements is wavelength-dependent [31], with a maximum, according to our calculations, of 7 mm at 1070 nm, which limits the measurements to the most superficial part of the liver tissue. Although steatosis heterogeneity can be significant [41], we have found nothing implying tissue structure is inhomogeneously distributed regarding the parenchyma depth when making scattered measurements of the liver surface. In our measurements, liver parenchyma composition was the same at the surface as compared with cross-section. Thus, scattered surface measurements are proposed to be representative of the normal liver. However, we have not analyzed severe pathology such as steatosis and fibrosis, which remains to be investigated further.

Previous DRS studies on human liver tissue have shown that liver tissue contains more blood and fat than tumor tissue [14,16]. This is consistent with the findings of the present study and is probably due to normal liver tissue being extremely well vascularized [16]. As shown in Fig. 3, there is a difference in diffuse reflectance spectra between tumor and liver tissue. This is particularly evident in the wavelength range between 500 and 900 nm where hemoglobin and bile are the dominant chromophores [16]. In the present study, liver parenchyma could be distinguished from that of tumors with high certainty (Fig. 4), similar to previous results [14,16]. However, the future purpose is not to detect tumors with this method, but to evaluate liver parenchymal damages such as steatosis, steatohepatitis and sinusoidal obstruction syndrome. These types of damage are common after preoperative chemotherapy and have been shown to increase postoperative complications and worsen long-term prognosis after liver resection for colorectal metastases [3,7,42-44]. Another possible use is in the setting of

orthotopic liver transplantation for assessment of fatty liver grafts [10]. It has been shown that >30 % hepatic steatosis is associated with decreased graft survival [45]. Hence, a reliable tool for intraoperative evaluation of liver steatosis is required.

Limitations to the method of DRS surface measurements consist mainly of a potential alteration of parenchyma composition due to pressure from the probe. To resolve this, a custom-made probe cylinder (Fig. 2) was used in order to distribute tissue pressure more consistently and the probe was only gently applied to the liver surface with as little pressure as possible. In an experimental study on skin the impact of contact pressure-induced spectral changes was investigated, showing decreased reflectance with the applied contact pressure [46].

Although the included number of patients in this study was small, the total number of collected DRS spectra was high, implying reliability of the data. As this study was an ex-vivo study and absorption coefficients vary slightly with temperature there is a possibility that the measurements will result in marginally different values in an in-vivo setting. To minimize this possibility, the measurements were made in the operating theatre directly after the liver specimen was resected in order to enable measurements on tissue as close to body temperature as possible.

Conclusion

This study shows that it is possible to manage DRS measurements through the liver capsule and that surface DRS measurements are representative of the whole liver. The method could distinguish between tumor and liver tissue on all declared parameters. The results are consistent with earlier published data on the combination of liver chromophores. The results encourage us to proceed with in-vivo measurements for further quantification of liver composition and assessment of parenchymal damage such as steatosis and fibrosis grade.

Acknowledgements

This research was partly financially supported by a grant from the Erik and Angelica Sparre research foundation and the Royal Physiographic Society of Lund.

References

1 Brouquet A, Benoist S, Julie C, Penna C, Beauchet A, Rougier P, Nordlinger B: Risk factors for chemotherapy-associated liver injuries: A multivariate analysis of a group of 146 patients with colorectal metastases. Surgery 2009;145:362-371.
2 Fernandez FG, Ritter J, Goodwin JW, Linehan DC, Hawkins WG, Strasberg SM: Effect of steatohepatitis associated with irinotecan or oxaliplatin pretreatment on resectability of hepatic colorectal metastases. Journal of the American College of Surgeons 2005;200:845-853.
3 Vauthey JN, Pawlik TM, Ribero D, Wu TT, Zorzi D, Hoff PM, Xiong HQ, Eng C, Lauwers GY, Mino-Kenudson M, Risio M, Muratore A, Capussotti L, Curley SA, Abdalla EK: Chemotherapy regimen predicts steatohepatitis and an increase in 90-day mortality after surgery for hepatic colorectal metastases. J Clin Oncol 2006;24:2065-2072.
4 Bohte AE, van Werven JR, Bipat S, Stoker J: The diagnostic accuracy of us, ct, mri and 1h-mrs for the evaluation of hepatic steatosis compared with liver biopsy: A meta-analysis. European radiology 2011;21:87-97.
5 Levene AP, Goldin RD: The epidemiology, pathogenesis and histopathology of fatty liver disease. Histopathology 2012;61:141-152.
6 Lucero C, Brown RS: Noninvasive measures of liver fibrosis and severity of liver disease. Gastroenterol Hepatol 2016;12:33-40.
7 Rubbia-Brandt L, Mentha G, Terris B: Sinusoidal obstruction syndrome is a major feature of hepatic lesions associated with oxaliplatin neoadjuvant chemotherapy for liver colorectal metastases. Journal of the American College of Surgeons 2006;202:199-200.
8 Park S, Kim HY, Kim H, Park JH, Kim JH, Kim KH, Kim W, Choi IS, Jung YJ, Kim JS: Changes in noninvasive liver fibrosis indices and spleen size during chemotherapy: Potential markers for oxaliplatin-induced sinusoidal obstruction syndrome. Medicine (United States) 2016;95
9 Evers DJ, Nachabe R, Klomp HM, van Sandick JW, Wouters MW, Lucassen GW, Hendriks BH, Wesseling J, Ruers TJ: Diffuse reflectance spectroscopy: A new guidance tool for improvement of biopsy procedures in lung malignancies. Clinical lung cancer 2012;13:424-431.
10 Evers DJ, Nachabe R, Vranken Peeters MJ, van der Hage JA, Oldenburg HS, Rutgers EJ, Lucassen GW, Hendriks BH, Wesseling J, Ruers TJ: Diffuse reflectance spectroscopy: Towards clinical application in breast cancer. Breast cancer research and treatment 2013;137:155-165.
11 Murphy BW, Webster RJ, Turlach BA, Quirk CJ, Clay CD, Heenan PJ, Sampson DD: Toward the discrimination of early melanoma from common and dysplastic nevus using fiber optic diffuse reflectance spectroscopy. Journal of biomedical optics 2005;10:064020.
12 Repez A, Oroszy D, Arnez ZM: Continuous postoperative monitoring of cutaneous free flaps using near infrared spectroscopy. Journal of plastic, reconstructive & aesthetic surgery : JPRAS 2008;61:71-77.
13 Langhout GC, Spliethoff JW, Schmitz SJ, Aalbers AG, van Velthuysen MF, Hendriks BH, Ruers TJ, Kuhlmann KF: Differentiation of healthy and malignant tissue in colon cancer patients using optical spectroscopy: A tool for image-guided surgery. Lasers in surgery and medicine 2015
14 Evers DJ, Nachabé R, Hompes D, van Coevorden F, Lucassen GW, Hendriks BH, van Velthuysen ML, Wesseling J, Ruers TJ: Optical sensing for tumor detection in the liver. European journal of surgical oncology : the journal of the European Society of Surgical Oncology and the British Association of Surgical Oncology 2013;39:68-75.

15 Evers DJ, Westerkamp AC, Spliethoff JW, Pully VV, Hompes D, Hendriks BH, Prevoo W, van Velthuysen ML, Porte RJ, Ruers TJ: Diffuse reflectance spectroscopy: Toward real-time quantification of steatosis in liver. Transpl Int 2015;28:465-474.
16 Nachabe R, Evers DJ, Hendriks BH, Lucassen GW, van der Voort M, Wesseling J, Ruers TJ: Effect of bile absorption coefficients on the estimation of liver tissue optical properties and related implications in discriminating healthy and tumorous samples. Biomedical optics express 2011;2:600-614.
17 Jayyosi C, Coret M, Bruyere-Garnier K: Characterizing liver capsule microstructure via in situ bulge test coupled with multiphoton imaging. Journal of the mechanical behavior of biomedical materials 2016;54:229-243.
18 Jacques SL: Optical properties of biological tissues: A review (vol 58, pg r37, 2013). Physics in medicine and biology 2013;58:5007-5008.
19 Nachabe R, Evers DJ, Hendriks BHW, Lucassen GW, van der Voort M, Wesseling J, Ruers TJM: Effect of bile absorption coefficients on the estimation of liver tissue optical properties and related implications in discriminating healthy and tumorous samples. Biomedical Optics Express 2011;2:600-614.
20 Hosoyamada Y, Kurihara H, Sakai T: Ultrastructural localisation and size distribution of collagen fibrils in glisson's sheath of rat liver: Implications for mechanical environment and possible producing cells. Journal of anatomy 2000;196:327-340.
21 Van Veen R, Verkruysse W, Sterenborg H: Diffuse-reflectance spectroscopy from 500 to 1060 nm by correction for inhomogeneously distributed absorbers. Opt Lett 2002;27:246-248.
22 Nachabé R, Hendriks BHW, van der Voort M, Desjardins AE, Sterenborg HJCM: Estimation of biological chromophores using diffuse optical spectroscopy: Benefit of extending the uv-vis wavelength range to include 1000 to 1600 nm. Biomed Opt Express 2010;1:1432-1442.
23 Zijlstra WG, Buursma A, van Assendelft OW: Visible and near infrared absorption spectra of human and animal haemoglobin: Determination and application. VSP, 2000.
24 Nachabé R, Hendriks BHW, Desjardins AE, van der Voort M, van der Mark MB, Sterenborg HJCM: Estimation of lipid and water concentrations in scattering media with diffuse optical spectroscopy from 900 to1600 nm. Journal of Biomedical Optics 2010;15:37015.
25 Taroni P, Bassi A, Comelli D, Farina A, Cubeddu R, Pifferi A: Diffuse optical spectroscopy of breast tissue extended to 1100nm. Journal of Biomedical Optics 2009;14:054030-054030-054037.
26 Nachabe R, Evers DJ, Hendriks BHW, Lucassen GW, van der Voort M, Rutgers EJ, Peeters M-JV, Van der Hage JA, Oldenburg HS, Wesseling J, Ruers TJM: Diagnosis of breast cancer using diffuse optical spectroscopy from 500 to 1600 nm: Comparison of classification methods. Journal of Biomedical Optics 2011;16
27 Van Veen R, Sterenborg HJ, Pifferi A, Torricelli A, Chikoidze E, Cubeddu R: Determination of visible near-ir absorption coefficients of mammalian fat using time-and spatially resolved diffuse reflectance and transmission spectroscopy. Journal of biomedical optics 2005;10:054004-054004-054006.
28 Hale GM, Querry MR: Optical constants of water in the 200-nm to 200-μm wavelength region. Appl Optics 1973;12:555-563.
29 D'Alessandro AM, Kalayoglu M, Sollinger HW, Hoffmann RM, Reed A, Knechtle SJ, Pirsch JD, Hafez GR, Lorentzen D, Belzer FO: The predictive value of donor liver biopsies for the development of primary nonfunction after orthotopic liver transplantation. Transplantation 1991;51:157-163.

30 Weibel ER, Gomez DM: A principle for counting tissue structures on random sections. Journal of applied physiology 1962;17:343-348.
31 Farrell TJ, Patterson MS, Wilson B: A diffusion theory model of spatially resolved, steady-state diffuse reflectance for the noninvasive determination of tissue optical properties in vivo. Medical physics 1992;19:879-888.
32 Nachabe R, Hendriks BH, van der Voort M, Desjardins AE, Sterenborg HJ: Estimation of biological chromophores using diffuse optical spectroscopy: Benefit of extending the uv-vis wavelength range to include 1000 to 1600 nm. Biomedical optics express 2010;1:1432-1442.
33 Nachabé R, Hendriks BHW, Desjardins AE, Van Der Voort M, Van Der Mark MB, Sterenborg HJCM: Estimation of lipid and water concentrations in scattering media with diffuse optical spectroscopy from 900 to 1600 nm. Journal of biomedical optics 2010;15
34 Zonios G, Bassukas I, Dimou A: Comparative evaluation of two simple diffuse reflectance models for biological tissue applications. Applied optics 2008;47:4965-4973.
35 Amelink A, Robinson DJ, Sterenborg HJ: Confidence intervals on fit parameters derived from optical reflectance spectroscopy measurements. Journal of biomedical optics 2008;13:054044.
36 Goetz M, Deris I, Vieth M, Murr E, Hoffman A, Delaney P, Galle PR, Neurath MF, Kiesslich R: Near-infrared confocal imaging during mini-laparoscopy: A novel rigid endomicroscope with increased imaging plane depth. Journal of hepatology 2010;53:84-90.
37 Robertson EG, Baxter G: Tumour seeding following percutaneous needle biopsy: The real story! Clinical radiology 2011;66:1007-1014.
38 McIntosh LM, Summers R, Jackson M, Mantsch HH, Mansfield JR, Howlett M, Crowson AN, Toole JW: Towards non-invasive screening of skin lesions by near-infrared spectroscopy. The Journal of investigative dermatology 2001;116:175-181.
39 van Veen RL, Verkruysse W, Sterenborg HJ: Diffuse-reflectance spectroscopy from 500 to 1060 nm by correction for inhomogeneously distributed absorbers. Optics letters 2002;27:246-248.
40 Nilsson J, Eriksson S, Blind PJ, Rissler P, Sturesson C: Microcirculation changes during liver resection--a clinical study. Microvascular research 2014;94:47-51.
41 Noworolski SM, Lam MM, Merriman RB, Ferrell L, Qayyum A: Liver steatosis: Concordance of mr imaging and mr spectroscopic data with histologic grade. Radiology 2012;264:88-96.
42 Gomez D, Malik HZ, Bonney GK, Wong V, Toogood GJ, Lodge JP, Prasad KR: Steatosis predicts postoperative morbidity following hepatic resection for colorectal metastasis. The British journal of surgery 2007;94:1395-1402.
43 Peppercorn PD, Reznek RH, Wilson P, Slevin ML, Gupta RK: Demonstration of hepatic steatosis by computerized tomography in patients receiving 5-fluorouracil-based therapy for advanced colorectal cancer. British journal of cancer 1998;77:2008-2011.
44 Tamandl D, Klinger M, Eipeldauer S, Herberger B, Kaczirek K, Gruenberger B, Gruenberger T: Sinusoidal obstruction syndrome impairs long-term outcome of colorectal liver metastases treated with resection after neoadjuvant chemotherapy. Annals of surgical oncology 2011;18:421-430.
45 Chu MJJ, Dare AJ, Phillips ARJ, Bartlett ASJR: Donor hepatic steatosis and outcome after liver transplantation: A systematic review. J Gastrointest Surg 2015;19:1713-1724.
46 Cugmas B, Bregar M, Bürmen M, Pernuš F, Likar B: Impact of contact pressure-induced spectral changes on soft-tissue classification in diffuse reflectance spectroscopy: Problems and solutions. Journal of biomedical optics 2014;19

Figure legends

Fig 1. Schematic picture of DRS instrumentation consisting of a light source, a fiber optic contact probe, and two spectrometers connected to a computer.

Fig 2. Picture of the 10 mm diameter trifurcated probe attached to a custom made cylinder with a diameter of 25 mm, thereby minimizing pressure effects, stabilizing the probe, and removing the impact of ambient light.

Fig 3. Typical diffuse reflectance spectroscopy (DRS) spectra. Left: with (solid-line curve) and without (point-marked curve) capsule on liver tissue. Middle: surface (point-marked curve) and cross-section (solid-line curve) on liver tissue. Right: tumor without capsule (point-marked curve) and liver tissue with capsule (solid-line curve).

Fig 4. Boxplots of tissue parameters for liver versus tumor tissue. Outliers are displayed with a red + sign.

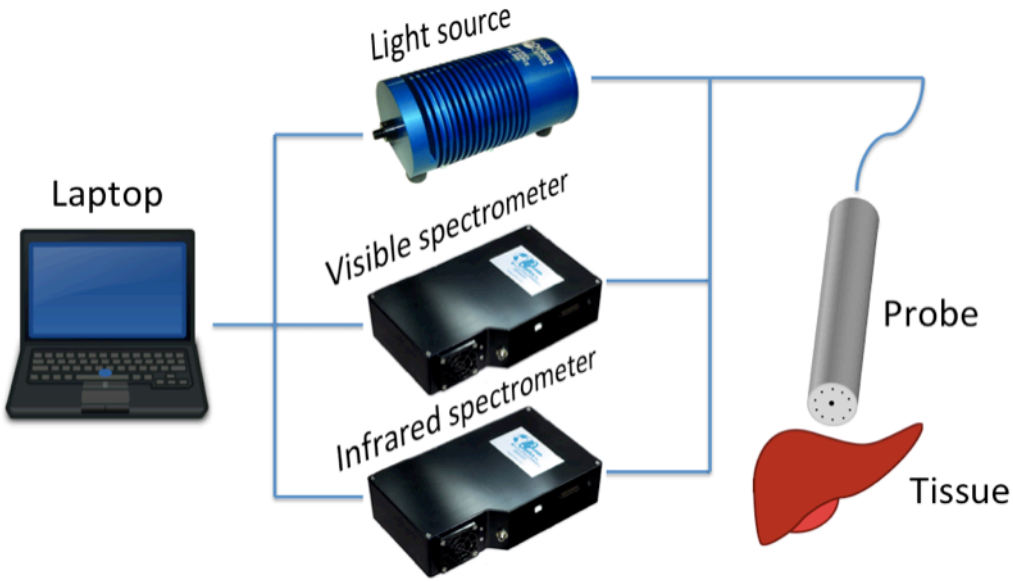
Light source
Laptop
Visible spectrometer
Infrared spectrometer
Probe
Tissue

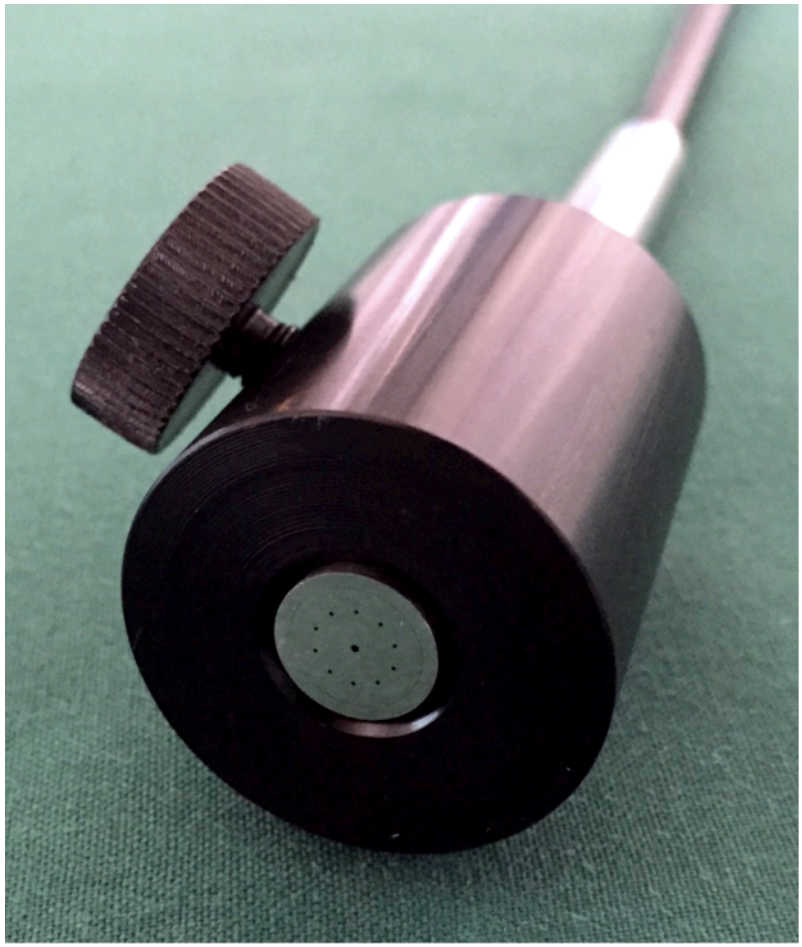

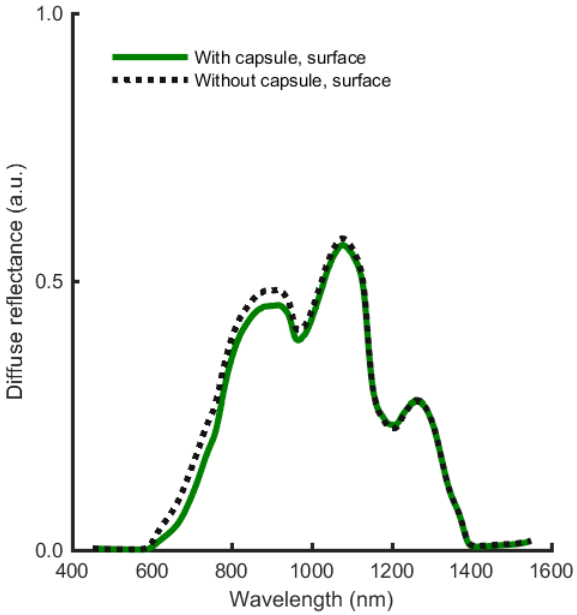
1.0
0.5
0.0
Diffuse reflectance (a.u.)
With capsule, surface
Without capsule, surface
400
600
800
1000
1200
1400
1600
Wavelength (nm)

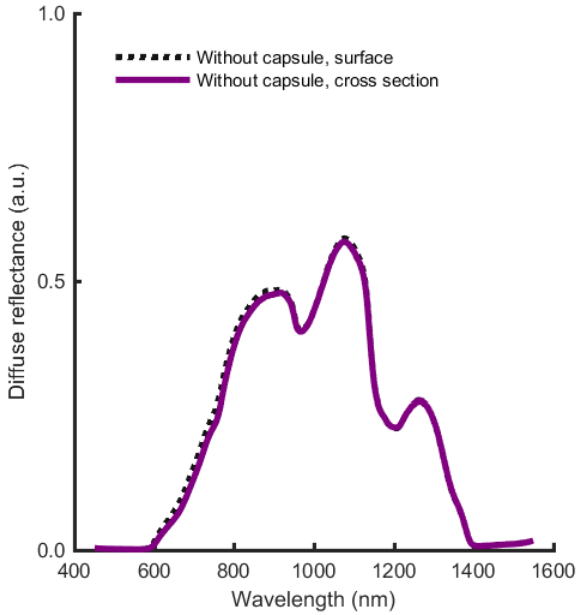
1.0
0.5
0.0
Diffuse reflectance (a.u.)
Without capsule, surface
Without capsule, cross section
400
600
800
1000
1200
1400
1600
Wavelength (nm)

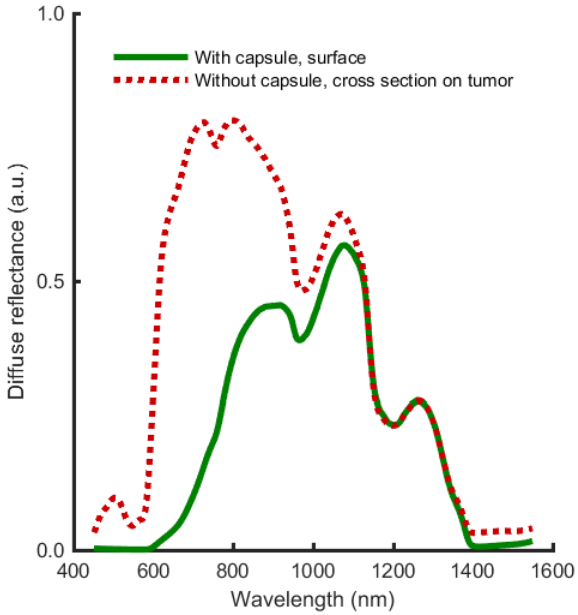
1.0
0.5
0.0
Diffuse reflectance (a.u.)
With capsule, surface
Without capsule, cross section on tumor
400
600
800
1000
1200
1400
1600
Wavelength (nm)

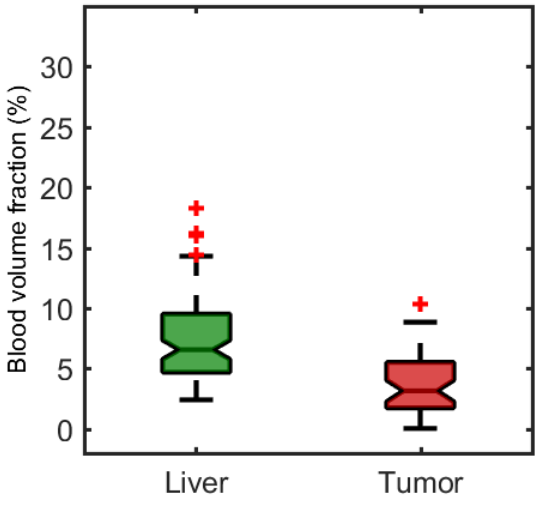
Blood volume fraction (%)
0
5
10
15
20
25
30
Liver
Tumor

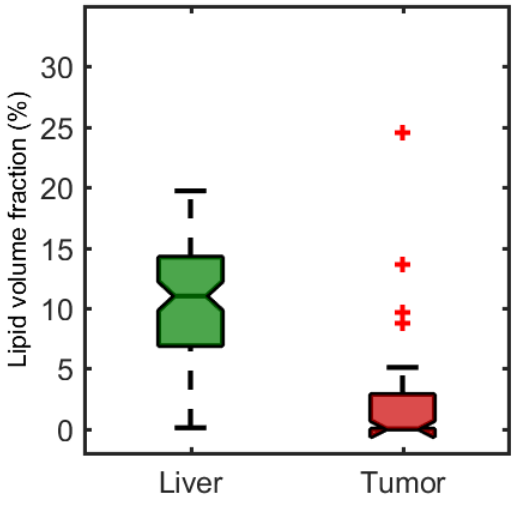
Lipid volume fraction (%)
0
5
10
15
20
25
30
Liver
Tumor

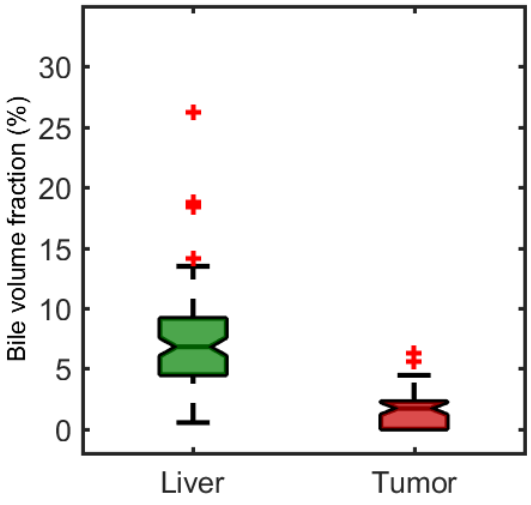
Bile volume fraction (%)
0
5
10
15
20
25
30
Liver
Tumor

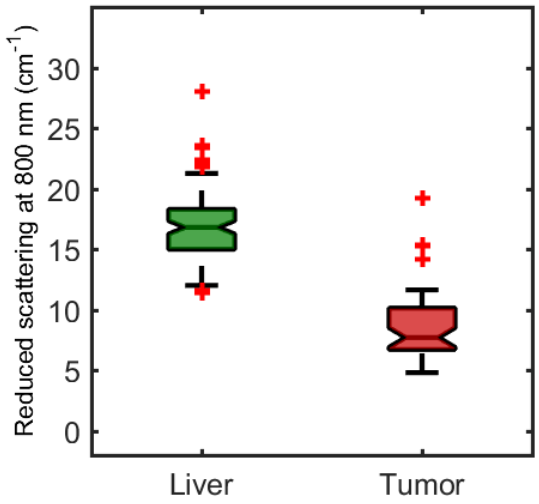
Reduced scattering at 800 nm (cm-1)
0
5
10
15
20
25
30
Liver
Tumor

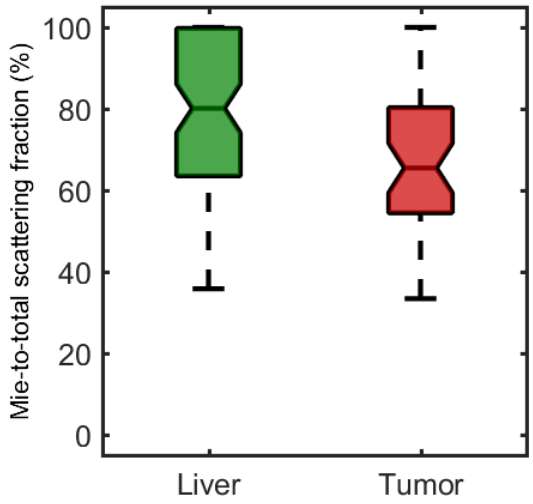
Mie-to-total scattering fraction (%)
0
20
40
60
80
100
Liver
Tumor

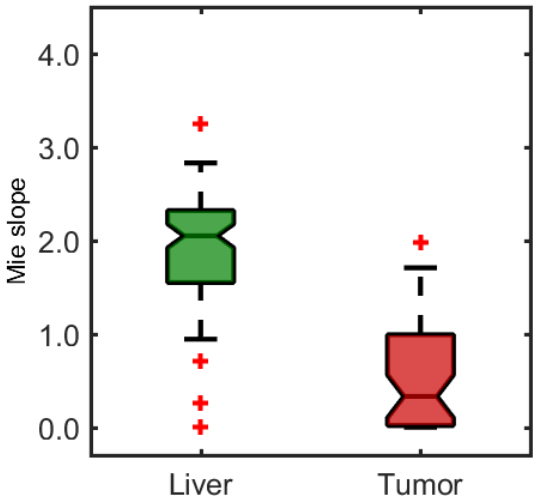
Mie slope
0.0
1.0
2.0
3.0
4.0
Liver
Tumor

Table 1. Patient characteristics.

No. of patients	18
Gender (male:female)	11:7
Age (years, range)	69.5 (45-78)
Diagnosis	
Colorectal liver metastases	14
Hepatocellular carcinoma	3
Duodenal cancer metastases	1

Table 2. DRS results with/without capsule and surface/cross-section measurements.

	Capsule		Depth	
	Difference with/without	P	Difference surface/cross-section	P
Reduced scattering coefficient at 800 nm (cm^{-1})	-0.33 (-1.28 – 0.46)	0.156	-0.51 (-1.14 – 0.63)	0.477
Mie to total scattering fraction (%)	0.83 (-12.97 – 9.78)	0.910	-0.02 (-11.48 – 3.19)	0.534
Blood volume fraction (%)	1.63 (0.75 – 2.77)	0.001	-0.58 (-1.78 – 1.20)	0.477
Lipid volume fraction (%)	-0.54 (-2.97 – 0.32)	0.100	-1.04 (-2.82 – 1.47)	0.477
Bile volume fraction (%)	-0.15 (-1.06 – 1.24)	0.955	-0.31 (-0.49 – 2.48)	0.374

Data are presented as median (interquartile range) calculated from the average differences in each patient. DRS, diffuse reflectance spectroscopy.